Electronic Supplementary Material (ESI) for Inorganic Chemistry Frontiers.

Supplementary information

Dimensional regulation of the aggregation-induced emission properties for complex

*Shuyu Wang, Lei Wang, Fang Fang, Xun Ma, Yuanyuan Guo, Ruidong Wang, Suoshu Zhang, Zhen Zhang, Lin Du * and Qi-Hua Zhao **

[*]Corresponding Authors

Key Laboratory of Medicinal Chemistry for Natural Resource, Ministry of Education and Yunnan Province, Yunnan Characteristic Plant Extraction Laboratory, School of Chemical Science and Technology, Yunnan University, Kunming, 650500, PR China

Email: lindu@ynu.edu.cn; qhzhao@ynu.edu.cn

Contents

Table S1. Crystallographic data for complexes **1–3**

	1	**2**	**3**
CCDC no.	2176115	2176116	2176117
empirical formula	$C_{202}H_{194}Eu_4N_6O_{39}$	$C_{60}H_{50}EuNO_7$	$C_{194}H_{154}Eu_2N_6O_{17}$
formula weight	3937.46	1048.97	3145.14
crystal system	Triclinic	Triclinic	Monoclinic
space group	$P\bar{1}$	$P\bar{1}$	$P2_1/c$
a (Å)	15.3422 (4)	9.3725 (4)	26.5569 (9)
b (Å)	15.6473 (3)	10.8238 (4)	15.4748 (6)
c (Å)	21.0007 (5)	25.4977 (9)	19.2252 (8)
α (°)	98.489 (1)	91.707 (1)	90
β (°)	97.894 (1)	98.209 (1)	96.452 (1)
γ (°)	111.685 (1)	106.989 (1)	90
V (Å^3)	4531.28 (19)	2441.42 (16)	7850.8 (5)
Z	1	2	2
ρ calc (mg m^{-3})	1.451	1.427	1.330
μ (mm^{-1})	1.45	1.34	0.86
F(000)	2012	1072	3244
Crystal size (mm^3)	0.043×0.014×0.006	0.074×0.012×0.007	0.023×0.012×0.009
Reflections collected	51650	24851	59060
Independent reflections	17794	8563	15775
GOF	1.05	1.04	1.07
R_1, wR_2 [I> 2σ(I)][b]	0.038,0.083	0.036,0.087	0.054,0.166
$\Delta\rho_{max}$, $\Delta\rho_{min}$ (e Å^{-3})	1.72,-0.81	1.11,-1.88	2.00,-1.45

Table S2. Selected bond distances and angles for complex **1**

bond distance	(Å)	bond distance	(Å)
Eu01−O11	2.539 (3)	O4−Eu02^{ii}	3.037 (3)
Eu01−O8	2.285 (3)	O14−Eu02^{iii}	2.337 (3)
Eu01−O10	2.458 (3)	O15−Eu02^{v}	2.421 (3)
Eu01−O7^{i}	2.493 (3)	O3−Eu02^{ii}	2.444 (2)
Eu01−O2^{ii}	2.509 (3)	O2−Eu01^{ii}	2.509 (3)
Eu01−O6^{i}	3.030 (3)	O6−Eu01^{i}	3.030 (3)
Eu01−O9^{iii}	2.368 (3)	O9−Eu01^{iii}	2.368 (3)
Eu01−O1^{ii}	2.453 (3)	O1−Eu01^{ii}	2.453 (3)
Eu01−O12	2.330 (3)	O13−Eu02^{i}	2.360 (3)
Eu01−C70^{ii}	2.827 (4)	C70−Eu01^{ii}	2.827 (4)
Eu01−C37^{i}	3.104 (4)	C37−Eu01^{i}	3.104 (4)
Eu02−Eu02^{ii}	4.1105 (4)	C59−Eu02^{ii}	3.118 (4)
Eu02−O4^{ii}	3.037 (3)	Eu02−O6	2.309 (3)
Eu02−O4	2.319 (3)	Eu02−O5	2.372 (3)
Eu02−O14^{iii}	2.337 (3)	Eu02−O13^{i}	2.360 (3)
Eu02−O15^{iv}	2.421 (3)	Eu02−C59^{ii}	3.118 (4)
Eu02−O3^{ii}	2.444 (2)		
angle	(°)	angle	(°)
O11−Eu01−O6^{i}	63.48 (8)	O4−Eu02−O13^{i}	84.81 (9)
O11−Eu01−C70^{ii}	141.30 (10)	O4^{ii}−Eu02−C59^{ii}	23.62 (8)
O11−Eu01−C37^{i}	71.69 (9)	O4−Eu02−C59^{ii}	103.99 (10)
O8−Eu01−O11	78.55 (9)	O14^{iii}−Eu02−Eu02^{ii}	60.87 (6)
O8−Eu01−O10	72.60 (9)	O14^{iii}−Eu02−O4^{ii}	62.41 (8)
O8−Eu01−O7^{i}	84.01 (9)	O14^{iii}−Eu02−O15^{iv}	127.19 (9)
O8−Eu01−O2^{ii}	125.32 (9)	O14^{iii}−Eu02−O3^{ii}	76.98 (9)
O8−Eu01−O6^{i}	121.73 (8)	O14^{iii}−Eu02−O5	74.31 (9)
O8−Eu01−O9^{iii}	104.27 (10)	O14^{iii}−Eu02−O13^{i}	144.99 (9)
O8−Eu01−O1^{ii}	74.18 (9)	O14^{iii}−Eu02−C59^{ii}	66.20 (9)
O8−Eu01−O12	145.19 (10)	O15^{iv}−Eu02−Eu02^{ii}	69.24 (6)
O8−Eu01−C70^{ii}	98.98 (11)	O15^{iv}−Eu02−O4^{ii}	66.79 (8)

O8−Eu01−C37^{i}	105.02 (10)	O15^{iv}−Eu02−O3^{ii}	78.23 (9)
O10−Eu01−O11	72.46 (9)	O15^{iv}−Eu02−C59^{ii}	73.33 (9)
O10−Eu01−O7^{i}	142.86 (9)	O3^{ii}−Eu02−Eu02^{ii}	79.61 (6)
O10−Eu01−O2^{ii}	146.54 (9)	O3^{ii}−Eu02−O4^{ii}	45.82 (8)
O10−Eu01−O6^{i}	127.35 (8)	O3^{ii}−Eu02−C59^{ii}	22.40 (9)
O10−Eu01−C70^{ii}	144.28 (10)	O6−Eu02−Eu02^{ii}	149.19 (7)
O10−Eu01−C37^{i}	143.76 (10)	O6−Eu02−O4^{ii}	115.39 (8)
O7^{i}−Eu01−O11	74.94 (9)	O6−Eu02−O4	163.90 (9)
O7^{i}−Eu01−O2^{ii}	70.58 (9)	O6−Eu02−O14^{iii}	109.91 (10)
O7^{i}−Eu01−O6^{i}	45.77 (8)	O6−Eu02−O15^{iv}	103.76 (9)
O7^{i}−Eu01−C70^{ii}	66.42 (10)	O6−Eu02−O3^{ii}	69.58 (9)
O7^{i}−Eu01−C37^{i}	22.64 (9)	O6−Eu02−O5	82.01 (10)
O2^{ii}−Eu01−O11	134.28 (9)	O6−Eu02−O13^{i}	82.91 (10)
O2^{ii}−Eu01−O6^{i}	71.00 (8)	O6−Eu02−C59^{ii}	91.92 (10)
O2^{ii}−Eu01−C70^{ii}	26.57 (9)	O5−Eu02−Eu02^{ii}	119.07 (7)
O2^{ii}−Eu01−C37^{i}	64.86 (9)	O5−Eu02−O4^{ii}	136.54 (9)
O6^{i}−Eu01−C37^{i}	23.85 (8)	O5−Eu02−O15^{iv}	151.27 (10)
O9^{iii}−Eu01−O11	142.68 (9)	O5−Eu02−O3^{ii}	129.12 (10)
O9^{iii}−Eu01−O10	73.09 (10)	O5−Eu02−C59^{ii}	135.17 (10)
O9^{iii}−Eu01−O7^{i}	142.14 (9)	O13^{i}−Eu02−Eu02^{ii}	122.29 (7)
O9^{iii}−Eu01−O2^{ii}	74.86 (9)	O13^{i}−Eu02−O4^{ii}	142.37 (9)
O9^{iii}−Eu01−O6^{i}	132.92 (8)	O13^{i}−Eu02−O15^{iv}	77.26 (9)
O9^{iii}−Eu01−O1^{ii}	73.49 (9)	O13^{i}−Eu02−O3^{ii}	137.17 (9)
O9^{iii}−Eu01−C70^{ii}	75.76 (10)	O13^{i}−Eu02−O5	75.56 (10)
O9^{iii}−Eu01−C37^{i}	138.96 (10)	O13^{i}−Eu02−C59^{ii}	147.97 (10)
O1^{ii}−Eu01−O11	139.95 (9)	C59^{ii}−Eu02−Eu02^{ii}	57.28 (7)
O1^{ii}−Eu01−O10	124.31 (9)	Eu02−O4−Eu02^{ii}	99.37 (8)
O1^{ii}−Eu01−O7^{i}	73.54 (9)	C59−O4−Eu02	171.4 (3)
O1^{ii}−Eu01−O2^{ii}	52.72 (8)	C59−O4−Eu02^{ii}	81.8 (2)
O1^{ii}−Eu01−O6^{i}	108.04 (8)	Eu01−O11−H11A	109.9
O1^{ii}−Eu01−C70^{ii}	26.57 (10)	Eu01−O11−H11B	110.1
O1^{ii}−Eu01−C37^{i}	87.62 (9)	C1−O14−Eu02^{iii}	142.7 (3)
O12−Eu01−O11	77.72 (9)	C1−O15−Eu02^{v}	129.7 (2)

O12−Eu01−O10	76.17 (9)	C30−O8−Eu01	165.1 (3)
O12−Eu01−O7^{i}	113.59 (9)	C59−O3−Eu02^{ii}	110.2 (2)
O12−Eu01−O2^{ii}	89.40 (9)	Eu01−O10−H10A	109.6
O12−Eu01−O6^{i}	67.84 (8)	Eu01−O10−H10B	110.1
O12−Eu01−O9^{iii}	80.55 (9)	C37−O7−Eu01^{i}	107.3 (2)
O12−Eu01−O1^{ii}	138.22 (9)	C70−O2−Eu01^{ii}	90.9 (2)
O12−Eu01−C70^{ii}	115.43 (11)	Eu02−O6−Eu01^{i}	122.67 (10)
O12−Eu01−C37^{i}	91.22 (10)	C37−O6−Eu01^{i}	81.3 (2)
C70^{ii}−Eu01−O6^{i}	87.06 (9)	C37−O6−Eu02	148.2 (3)
C70^{ii}−Eu01−C37^{i}	71.80 (11)	C30−O9−Eu01^{iii}	134.6 (2)
O4^{ii}−Eu02−Eu02^{ii}	33.82 (5)	C70−O1−Eu01^{ii}	93.4 (2)
O4−Eu02−Eu02^{ii}	46.80 (7)	C24−O12−Eu01	157.8 (3)
O4−Eu02−O4^{ii}	80.63 (8)	C87−O5−Eu02	138.3 (3)
O4−Eu02−O14^{iii}	75.15 (9)	C24−O13−Eu02^{i}	131.9 (2)
O4−Eu02−O15^{iv}	83.56 (9)	O2−C70−Eu01^{ii}	62.6 (2)
O4−Eu02−O3^{ii}	126.38 (9)	O1−C70−Eu01^{ii}	60.0 (2)
O4−Eu02−O5	84.87 (10)	C69−C70−Eu01^{ii}	162.0 (3)
O4−C59−Eu02^{ii}	74.6 (2)	O7−C37−Eu01^{i}	50.08 (19)
O3−C59−Eu02^{ii}	47.36 (17)	O6−C37−Eu01^{i}	74.8 (2)
C60−C59−Eu02^{ii}	163.5 (3)	C38−C37−Eu01^{i}	155.0 (3)

Symmetry codes: (i) -*x*, -*y*+1, -*z*+1; (ii) -*x*, -*y*+2, -*z*+1; (iii) -*x*+1, -*y*+1, -*z*+1; (iv) *x*-1, *y*+1, *z*; (v) *x*+1, *y*-1, *z*.

Table S3. Selected bond distances and angles for complex **2**

bond distance	(Å)	bond distance	(Å)
Eu01−O002^{i}	2.346 (4)	Eu01−O007	2.438 (4)
Eu01−O003^{ii}	2.328 (4)	Eu01−O008	2.320 (5)
Eu01−O004	2.288 (4)	O002−Eu01^{i}	2.346 (4)
Eu01−O005	2.280 (4)	O003−Eu01^{ii}	2.328 (4)
Eu01−O006	2.431 (4)		
angle	(°)	angle	(°)
O002^{i}–Eu01−O006	128.98 (14)	O004−Eu01−O008	88.62 (16)
O002^{i}–Eu01−O007	76.95 (14)	O005−Eu01−O002^{i}	85.89 (13)
O003^{ii}–Eu01−O002^{i}	155.59 (15)	O005−Eu01−O003^{ii}	94.14 (14)
O003^{ii}–Eu01−O006	75.32 (15)	O005−Eu01−O004	176.68 (14)
O003^{ii}–Eu01−O007	127.26 (15)	O005−Eu01−O006	87.00 (15)
O004−Eu01−O002^{i}	92.01 (13)	O005−Eu01−O007	94.84 (16)
O004−Eu01−O003^{ii}	86.71 (13)	O005−Eu01−O008	88.44 (16)
O004−Eu01−O006	96.32 (15)	O006−Eu01−O007	53.46 (14)
O004−Eu01−O007	87.18 (15)	O008−Eu01−O002^{i}	78.15 (15)
C00B−O003−Eu01^{ii}	148.7 (3)	O008−Eu01−O003^{ii}	77.44 (16)
C00B−O004−Eu01	165.0 (4)	O008−Eu01−O006	151.97 (16)
C00D−O005−Eu01	171.2 (4)	O008−Eu01−O007	154.57 (16)
C00L−O006−Eu01	93.5 (3)	C00D−O002−Eu01^{i}	135.3 (3)
C00L−O007−Eu01	93.3 (3)	C01A−O008−Eu01	158.7 (4)

Symmetry codes: (i) -*x*+1, -*y*+2, -*z*+1; (ii) -*x*+1, -*y*+1, -*z*+1.

Table S4. Selected bond distances and angles for complex **3**

bond distance	(Å)	bond distance	(Å)
Eu1−O4	2.299 (3)	Eu1−N1	2.629 (4)
Eu1−O2	2.475 (3)	Eu1−O9	2.321 (6)
Eu1−O6	2.352 (3)	Eu1−N2	2.623 (4)
Eu1−O1	2.398 (3)	Eu1−C19	2.834 (5)
Eu1−O3	2.456 (3)	Eu1−O8	2.390 (14)
angle	(°)	angle	(°)
O4−Eu1−O2	87.21 (11)	N2−Eu1−C19	76.48 (13)
O4−Eu1−O6	84.70 (12)	O8−Eu1−O2	124.4 (4)
O4−Eu1−O1	144.12 (11)	O8−Eu1−O1	68.3 (4)
O4−Eu1−O3	124.93 (12)	O8−Eu1−O3	92.9 (4)
O4−Eu1−N1	74.29 (11)	O8−Eu1−N1	137.6 (4)
O4−Eu1−O9	71.81 (19)	O8−Eu1−N2	144.9 (4)
O4−Eu1−N2	133.80 (12)	O8−Eu1−C19	109.7 (4)
O4−Eu1−C19	106.63 (13)	C27−O4−Eu1	159.0 (3)
O4−Eu1−O8	79.0 (4)	C19−O2−Eu1	92.7 (3)
O2−Eu1−N1	86.82 (11)	C61−O6−Eu1	141.0 (3)
O2−Eu1−N2	76.81 (12)	O9−Eu1−C19	90.9 (2)
O2−Eu1−C19	26.55 (12)	O3−Eu1−C19	26.62 (12)
O6−Eu1−O2	156.52 (11)	C19−O3−Eu1	93.5 (3)
O6−Eu1−O1	73.53 (11)	C6−N1−Eu1	121.0 (3)
O6−Eu1−O3	146.06 (12)	C7−N1−Eu1	121.2 (3)
O6−Eu1−N1	69.78 (11)	C96−O9−Eu1	151.9 (8)
O6−Eu1−N2	93.12 (12)	C11−N2−Eu1	121.3 (3)
O6−Eu1−C19	168.10 (13)	C60−N2−Eu1	121.1 (3)
O6−Eu1−O8	75.5 (4)	O2−C19−Eu1	60.7 (2)
O1−Eu1−O2	123.09 (11)	O3−C19−Eu1	59.9 (2)
O1−Eu1−O3	72.54 (11)	C3−C19−Eu1	178.4 (3)
O1−Eu1−N1	121.55 (12)	O9−Eu1−O2	102.1 (2)
O1−Eu1−N2	76.68 (12)	O9−Eu1−O6	96.3 (2)
O1−Eu1−C19	98.10 (13)	O9−Eu1−O1	82.4 (2)

O3−Eu1−O2	53.16 (11)	O9−Eu1−O3	80.4 (2)
O3−Eu1−N1	129.43 (11)	O9−Eu1−N1	144.37 (19)
O3−Eu1−N2	78.07 (12)	O9−Eu1−N2	153.59 (19)

Table S5. The viscosity of glycerol/DMA mixtures with different glycerol fractions (25℃).

f_g (%)	99	90	80	70	60	50	40	30	20	10
lg η	2.87	2.61	2.32	2.02	1.73	1.43	1.14	0.84	0.55	0.26

Table S6. Singlet-singlet electronic transitions for complex **3**.

Complex **3**	Functional	λ_{max} (nm)	f	Assignment	Active MO	Cts (%)
Absorption	CAM-B3LYP	327.91	0.802	π→π*	H→L+2	32.1%
					H-1→L+4	28.6%
					H→L+4	21.8%
					H-1→L+1	10.1%
Absorption	CAM-B3LYP	326.38	0.411	π→π*	H-2→L+3	92.0%
Absorption	CAM-B3LYP	335.93	0.147	π→σ*	H-1→L+4	19.5%
					H→L+4	13.0%
					H→L+1	10.5%
Absorption	CAM-B3LYP	272.10	0.403	π→π*	H→L+7	31.6%
					H-1→L+5	26.4%
					H→L+8	6.0%
Absorption	CAM-B3LYP	270.14	0.320	π→σ*	H-2→L+6	68.7%
					H-6→L+3	7.8%
Absorption	CAM-B3LYP	265.45	0.298	π→σ*	H-1→L+9	16.7%
					H→L+8	14.6%
					H-1→L+5	9.4%
					H-1→L+2	8.4%
					H-1→L+8	7.5%
					H-1→L+4	7.0%
					H→L+7	5.9%

Table S7. Angles between different benzene planes of complex **2** under different temperature.

Complex **2** (100K)		Complex **2** (298K)	
angle	(°)	angle	(°)
P1-P2	64.76	P1-P2	66.12
P1-P3	57.61	P1-P3	59.95
P1-P4	82.83	P1-P4	83.10
P5-P6	80.53	P5-P6	84.17
P5-P7	65.50	P5-P7	63.33
P5-P8	57.47	P5-P8	59.02

Table S8. Angles between different benzene planes of complex **3** under different temperature.

Complex **3** (100K)		Complex **3** (298K)	
angle	(°)	angle	(°)
P1-P2	89.90	P1-P2	87.41
P1-P3	57.51	P1-P3	63.86
P1-P4	59.23	P1-P4	61.04
P5-P6	73.11	P5-P6	76.77
P5-P7	64.73	P5-P7	70.82
P5-P8	60.76	P5-P8	61.85
P9-P10	86.62	P9-P10	83.39
P9-P11	72.83	P9-P11	70.68
P9-P12	57.05	P9-P12	59.28

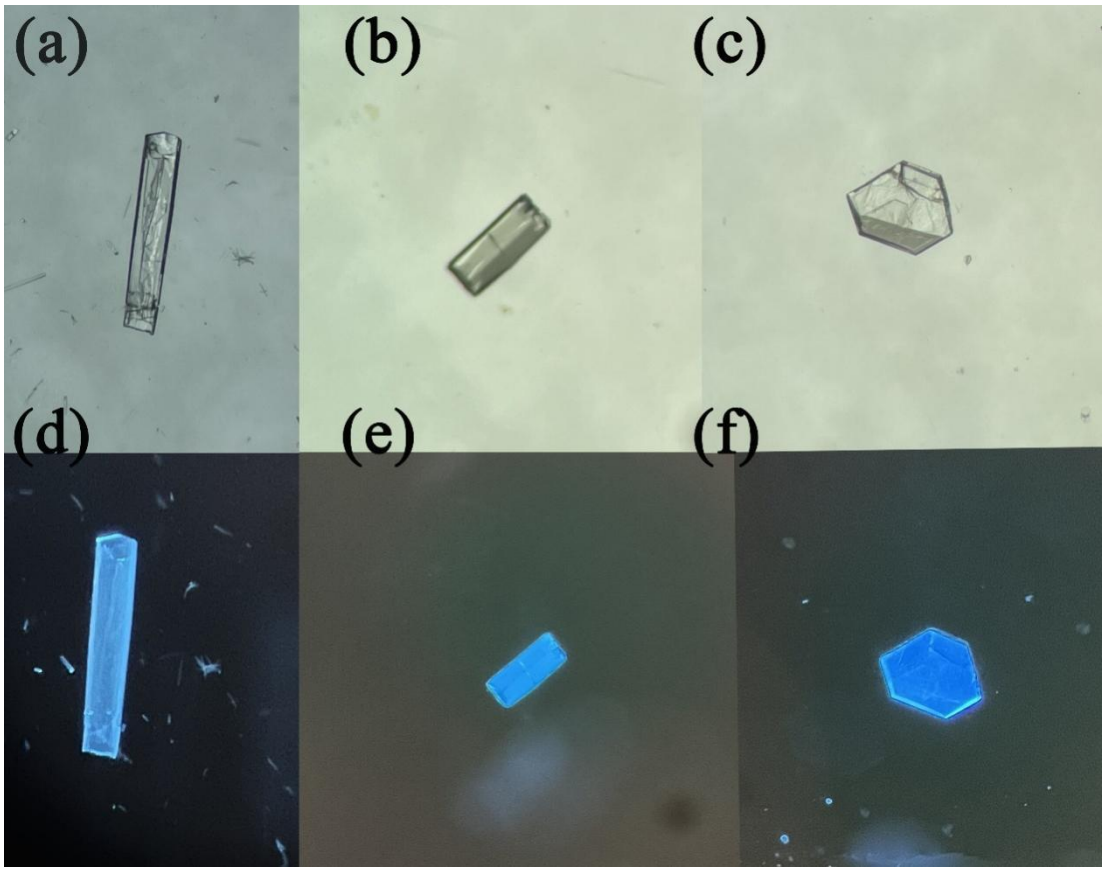

Fig. S1 The Crystal photo under sunlight (a), (b), (c) and under UV light (d), (e), (f).

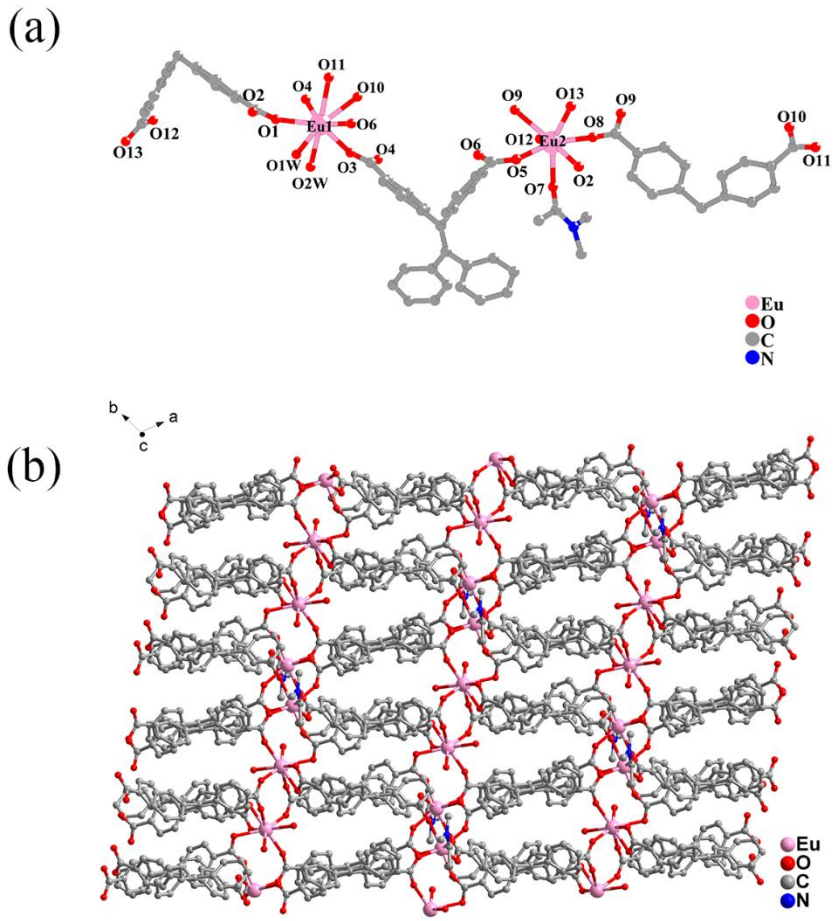

Fig. S2 (a) The coordination environment of complex **1**, (b) Two-dimensional planar structure of complex **1**. The hydrogen atom and solvent molecules has been omitted for clarity.

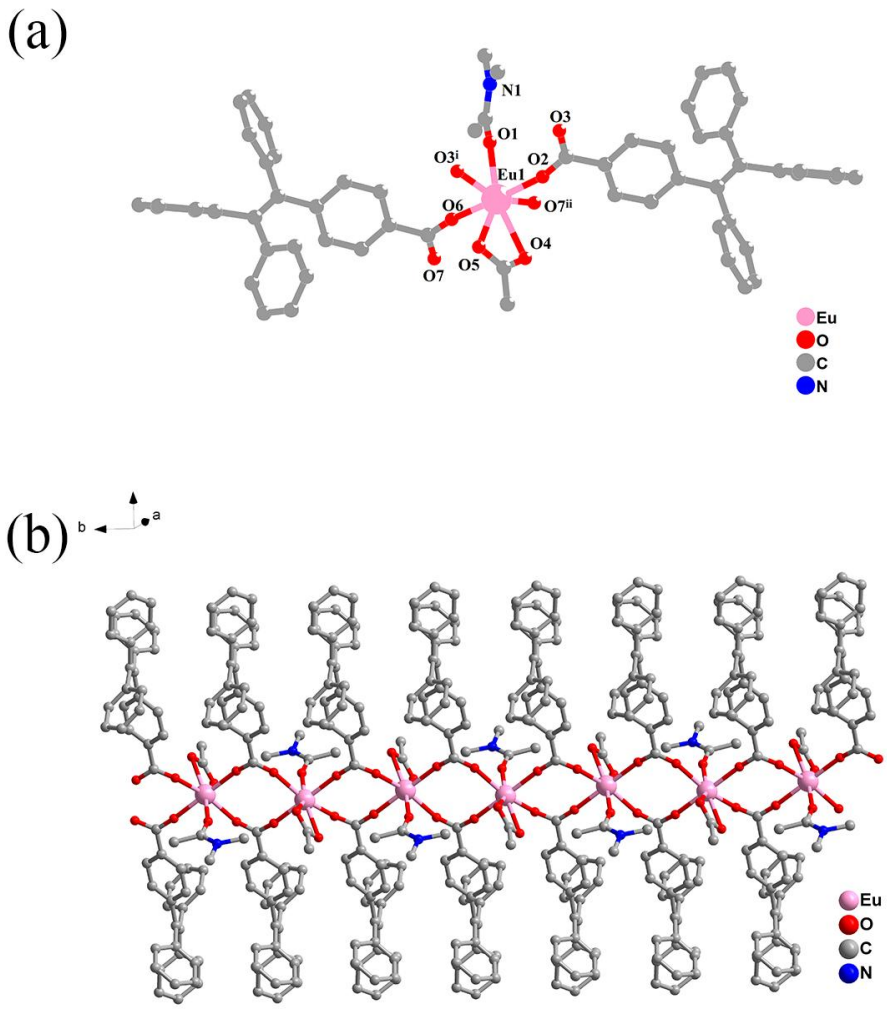

Fig. S3 (a) The coordination environment of complex **2**, (b) One-dimensional chain of complex **2**. The hydrogen atom and solvent molecules has been omitted for clarity.

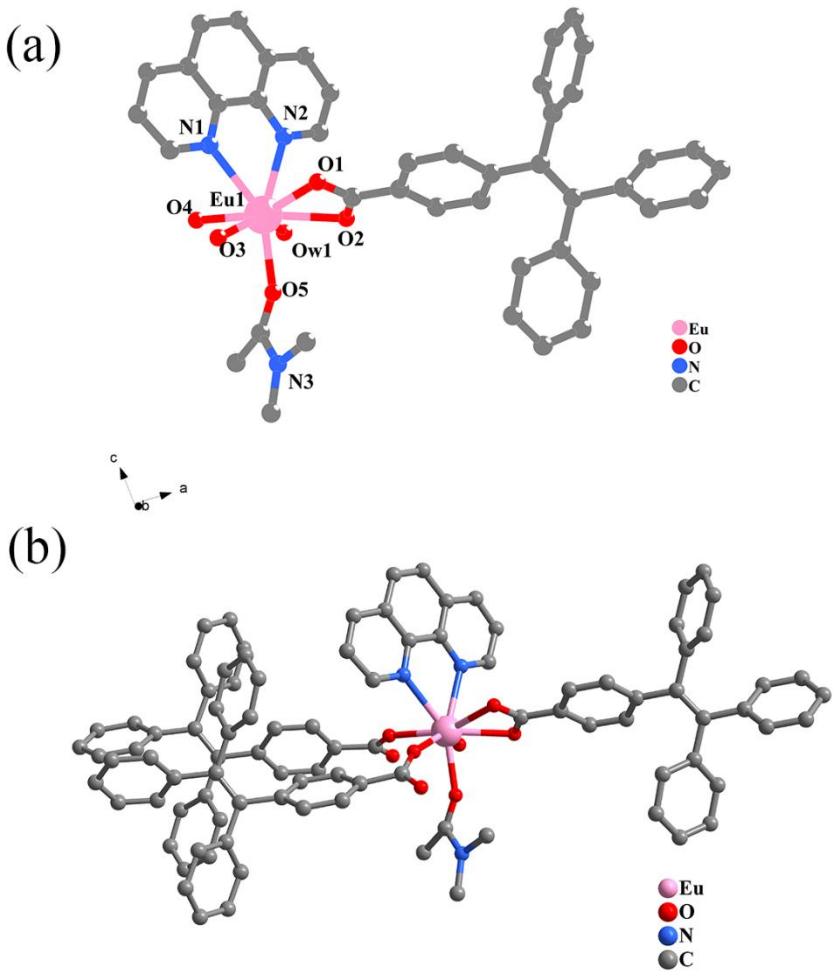

Fig. S4 (a) The coordination environment of complex **3**, (b) Zero-dimensional structure of complex **3**. The hydrogen atom and solvent molecules has been omitted for clarity.

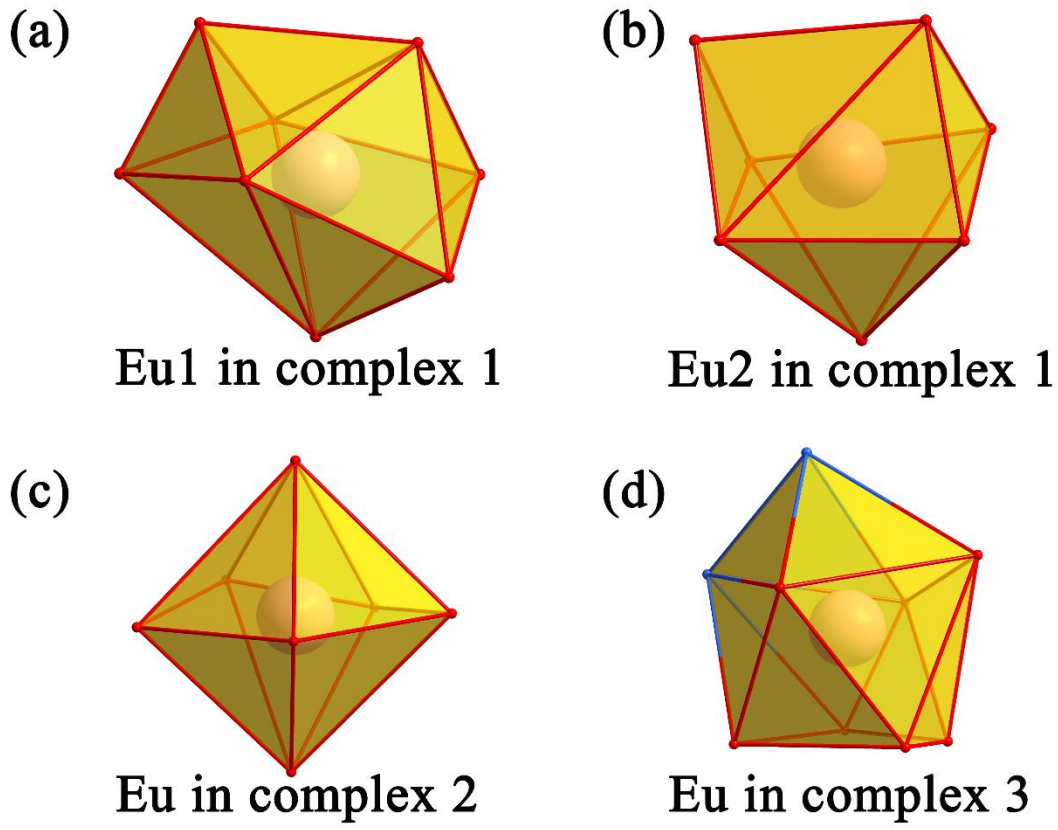

Fig. S5 Coordination configurations of Eu^{3+} in complex **1** (a) and (b), complex **2** (c) and complex **3** (d)

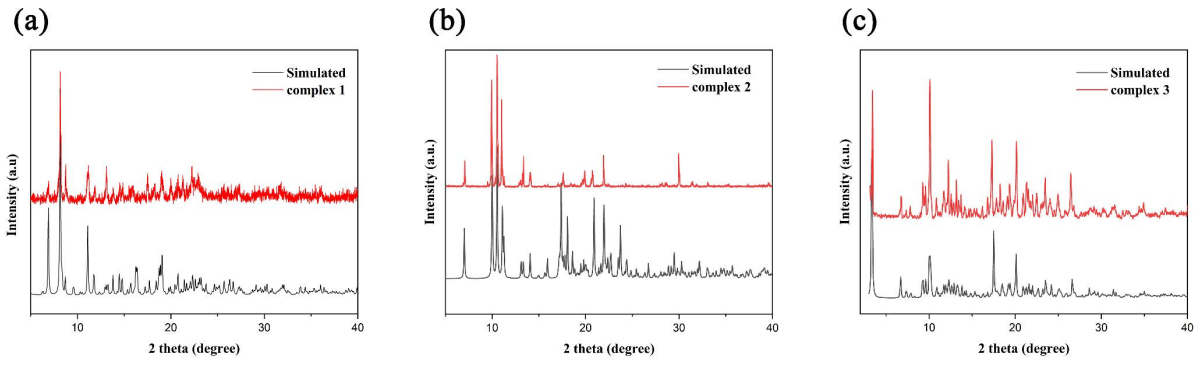

Fig. S6 PXRD patterns of complex **1** (a), complex **2** (b), and complex **3** (c). Where the black line is obtained by software simulation, and the red line is the result obtained by the actual test of the sample.

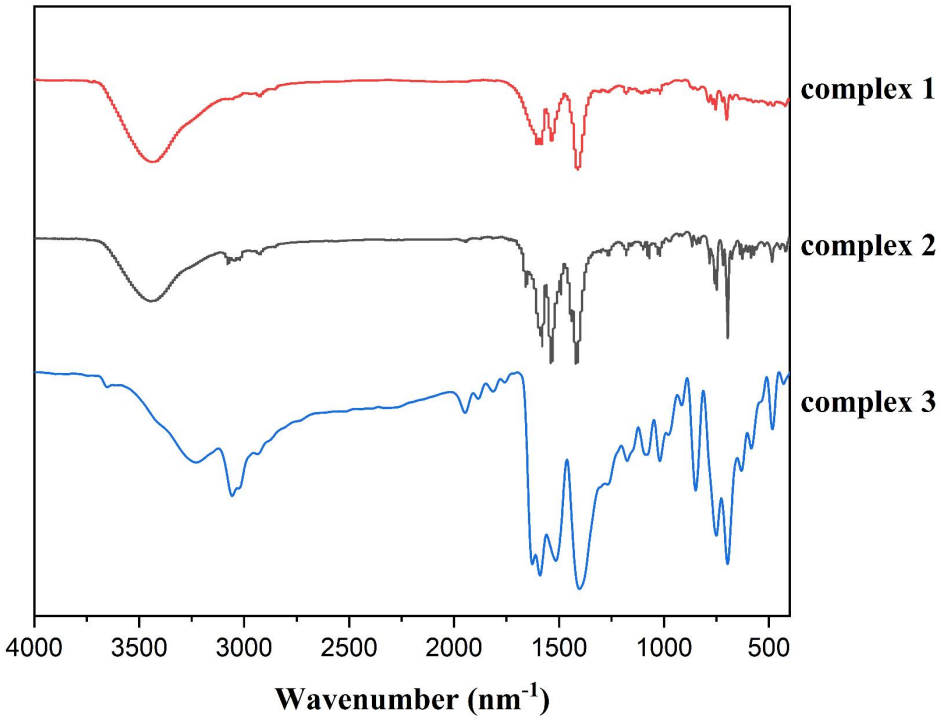

Fig. S7 FI-IR spectrum of complexes **1–3**

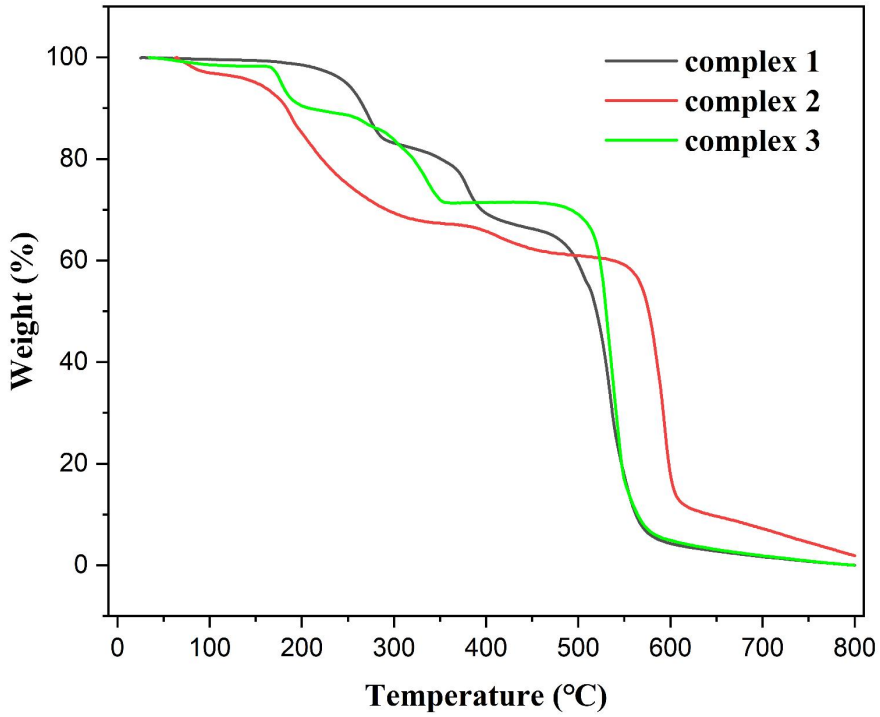

Fig. S8 Thermogravimetric analysis (TGA) curves of complexes **1–3**

In order to further study whether there are free solvent molecules or the number of free solvent molecules in the structure of complexes **1–3**, and at the same time to study the thermal stability of complexes **1–3**, we test the thermogravimetric curves of the complexes under a nitrogen atmosphere at a heating rate of 10 ℃/min in the range from room temperature to 800℃.

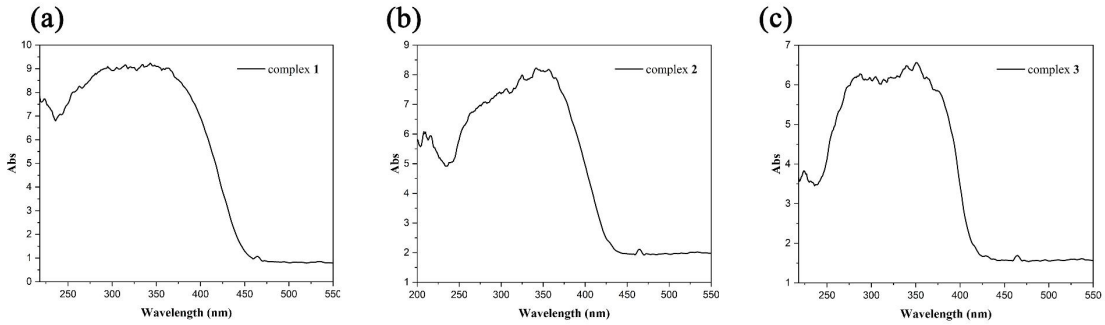

Fig. S9 UV-Visible absorption spectra of complex **1,** complex **2** and complex **3** in solid state.

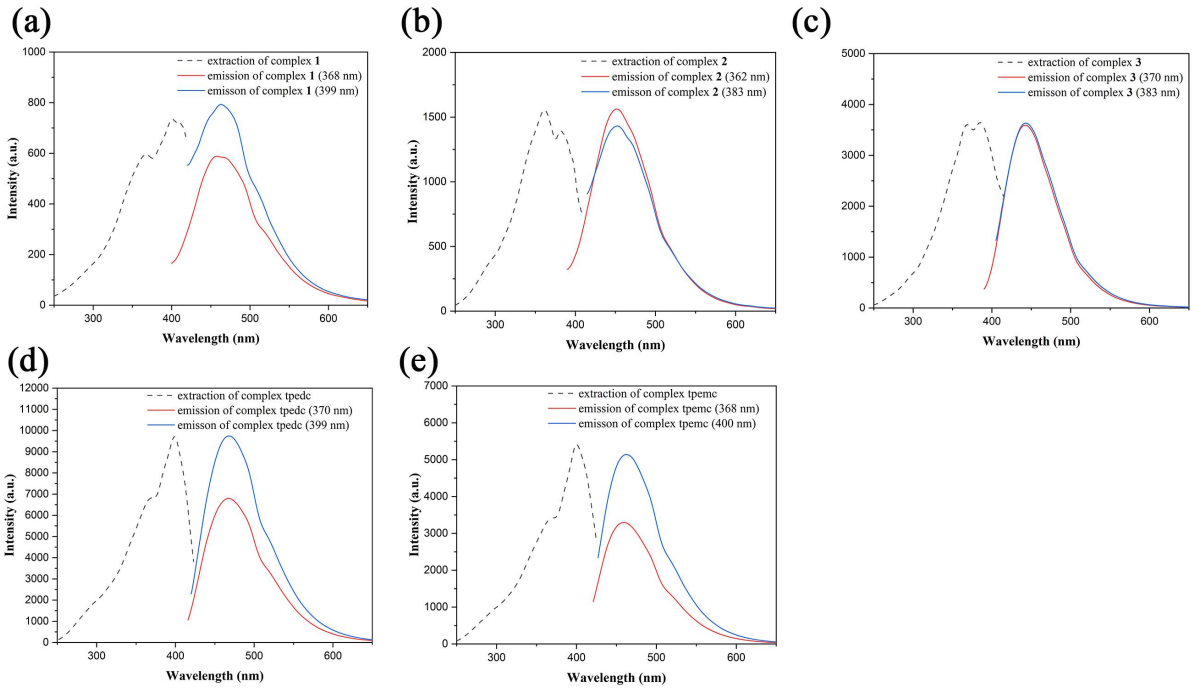

Fig. S10 Solid-state fluorescence excitation and emission spectra of complex **1** (a), the emission peaks are at 458 nm and 459 nm (when extraction wavelength at 368 nm and 399 nm); complex **2** (b), the emission peaks are both at 450 nm (when extraction wavelength at 362 nm and 383 nm); complex **3** (c), the emission peaks are both at 439 nm (when extraction wavelength at 370 nm and 383 nm); tpedc (d), the emission peaks are 467 nm and 468 nm (when extraction wavelength at 369 nm and 399 nm) and tpemc (e) the emission peaks are 462 nm and 464 nm (when extraction wavelength at 370 nm and 400 nm).

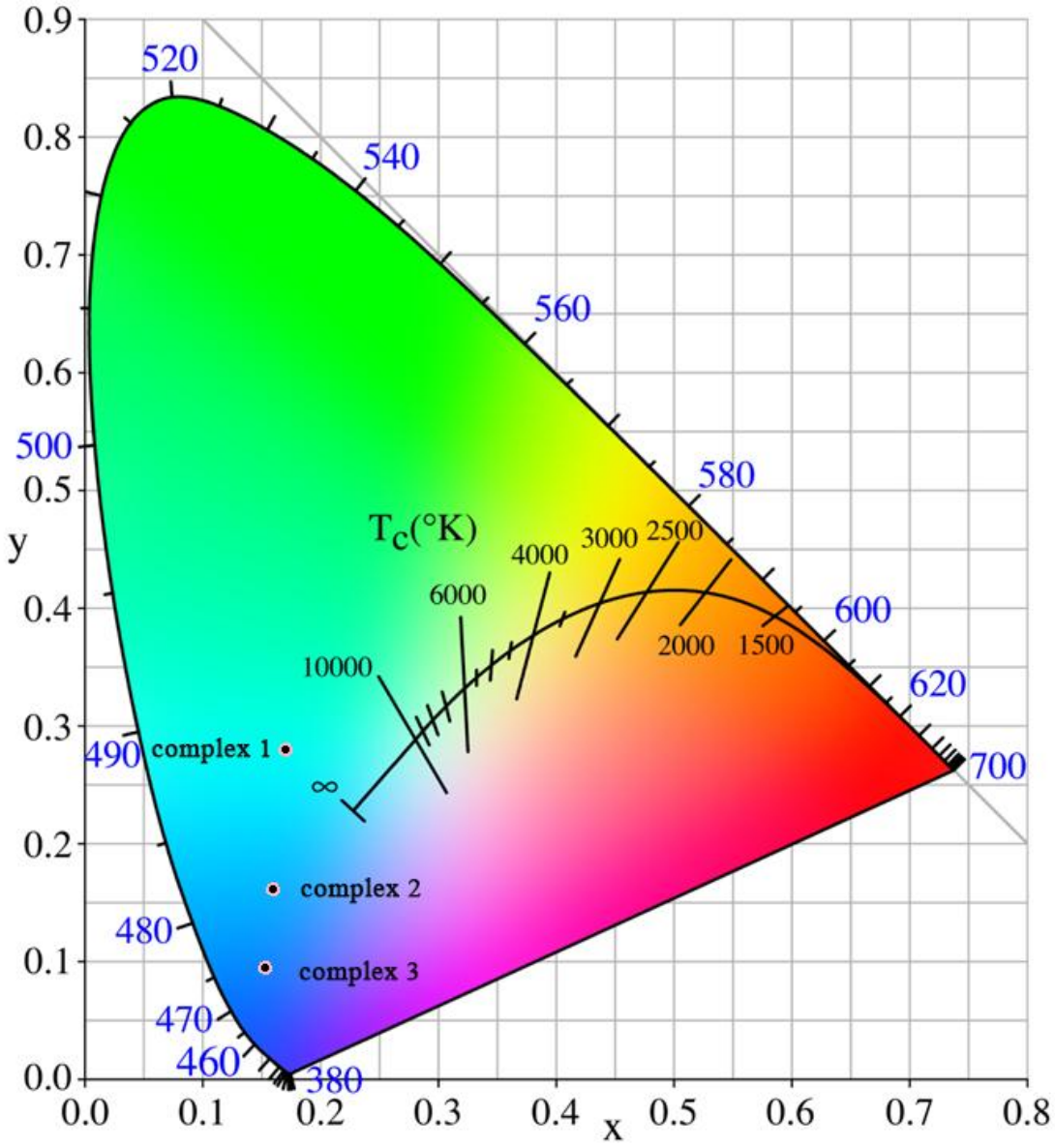

Fig. S11 CIE properties of complex **1**, complex **2** and complex **3** in solid state.

♦ Decay2 (Em).FL

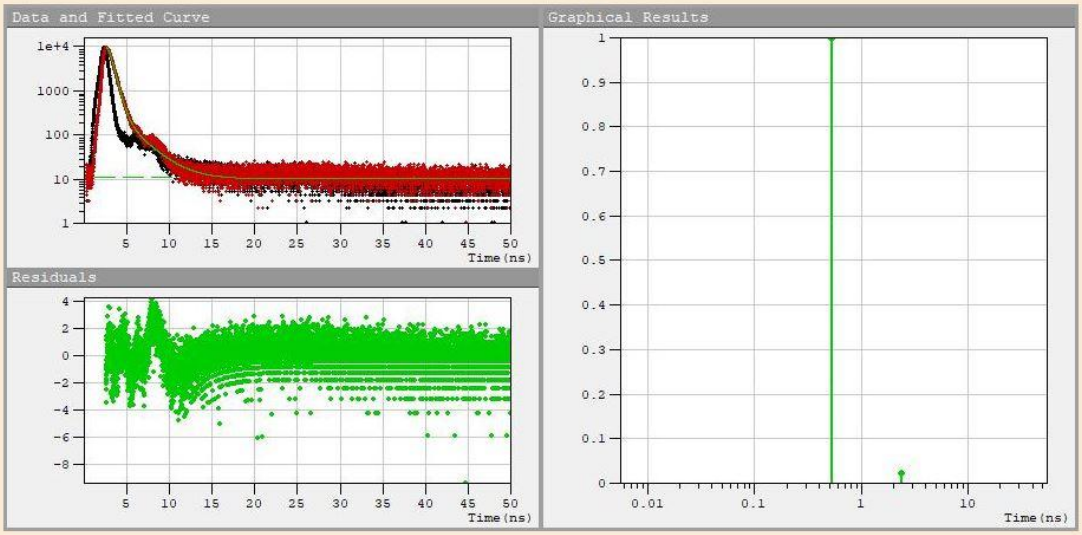

File: Decay2 (Em).FL

❖ **Exponential Components Analysis (Reconvolution)**

Fitting range : [394; 8192] channels

χ^2 : 1.455

	B_i	f_i	τ_i (ns)
1	0.0183	91.479	0.508
2	0.0004	8.521	2.290

Shift : -0.0816 ns

Decay Background : 10.428

IRF background : 92.100

Fig. S12 Fluorescence lifetime of complex **1**.

♦ Decay1 (Em).FL

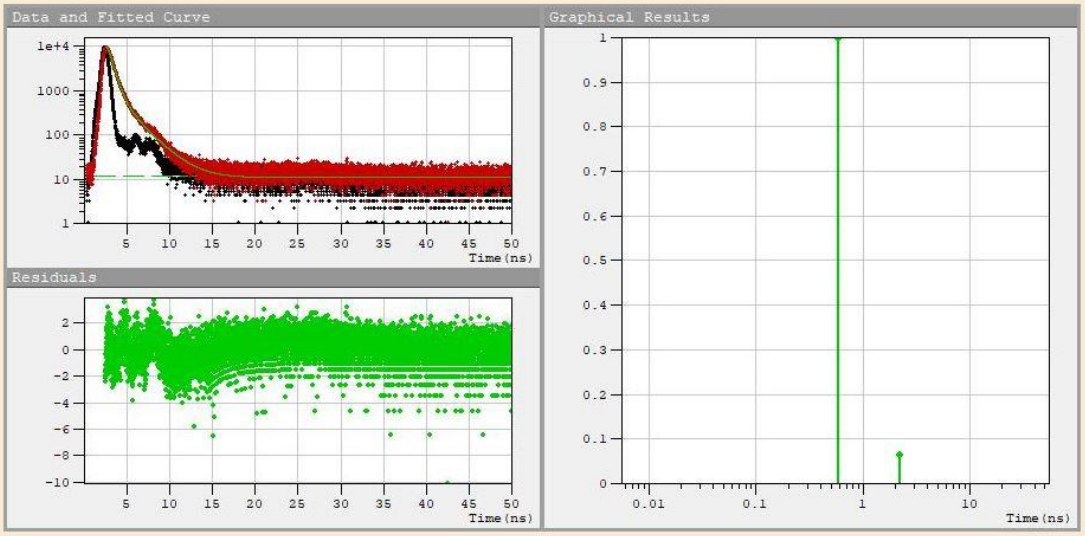

File: Decay1 (Em).FL

❖ **Exponential Components Analysis (Reconvolution)**

Fitting range : [379; 8192] channels

χ^2 : 1.384

	B_i	f_i	τ_i (ns)
1	0.0164	80.591	0.555
2	0.0010	19.409	2.138

Shift : -0.2025 ns

Decay Background : 11.102

IRF background : 62.100

Fig. S13 Fluorescence lifetime of complex **2**.

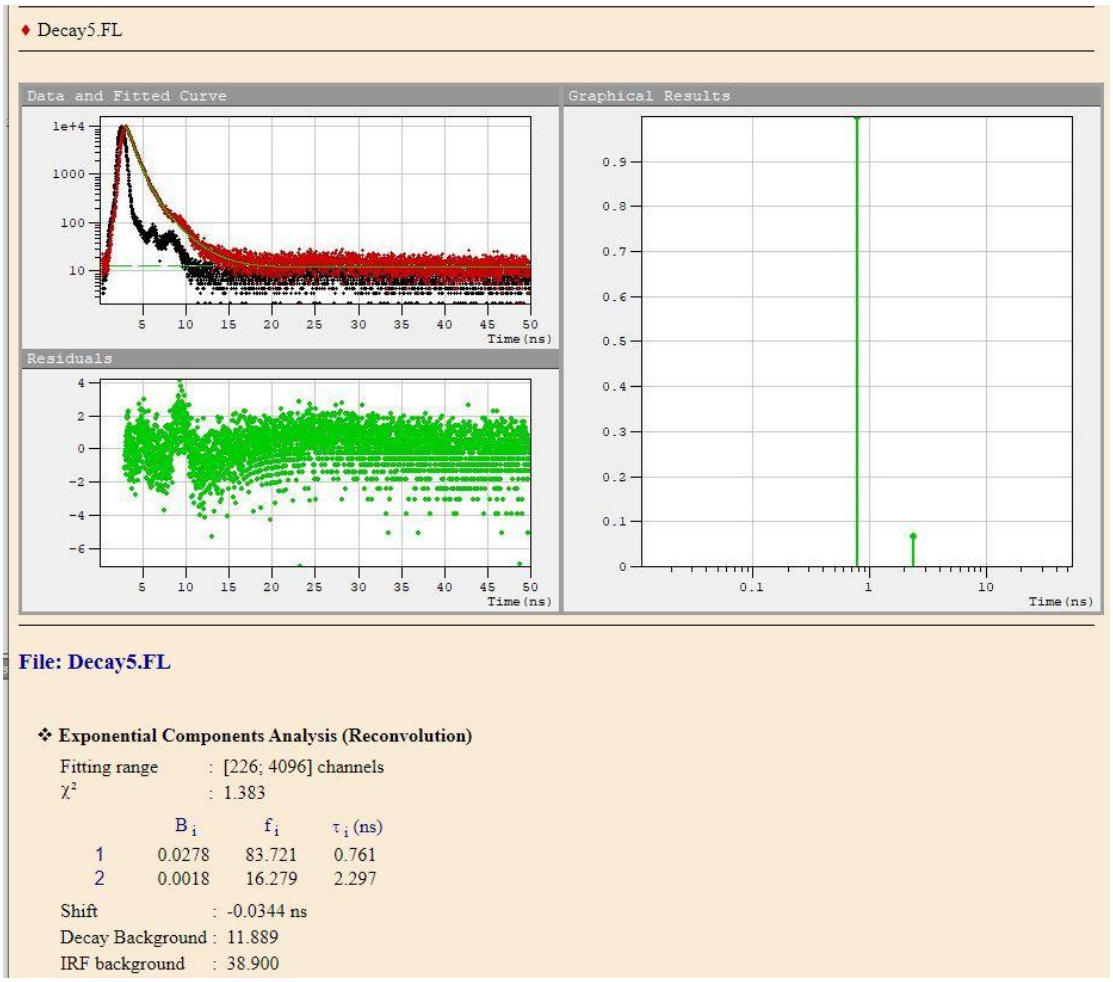

Fig. S14 Fluorescence lifetime of complex **3**.

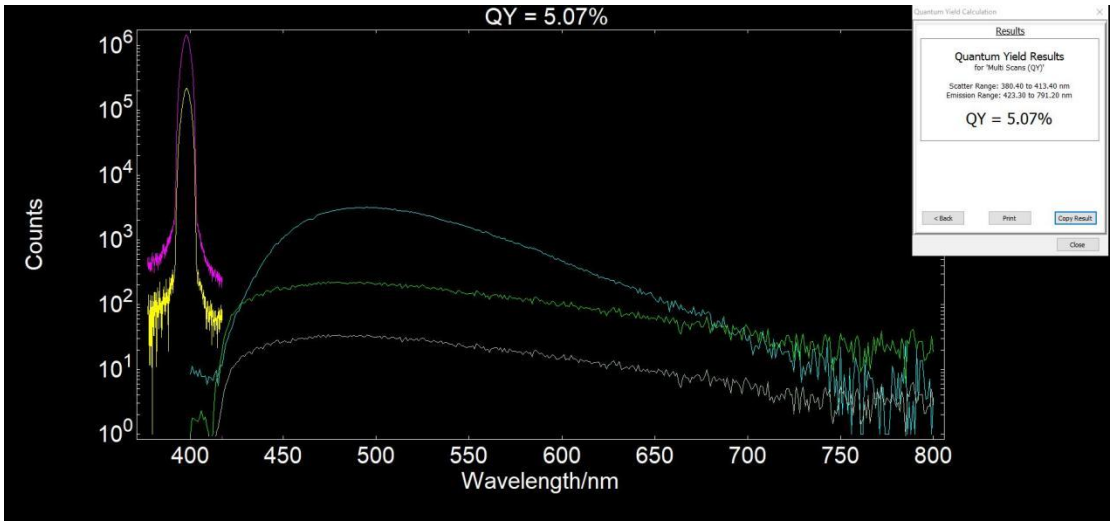

Fig. S15 Absolute fluorescence quantum yield of complex **1** in solid state.

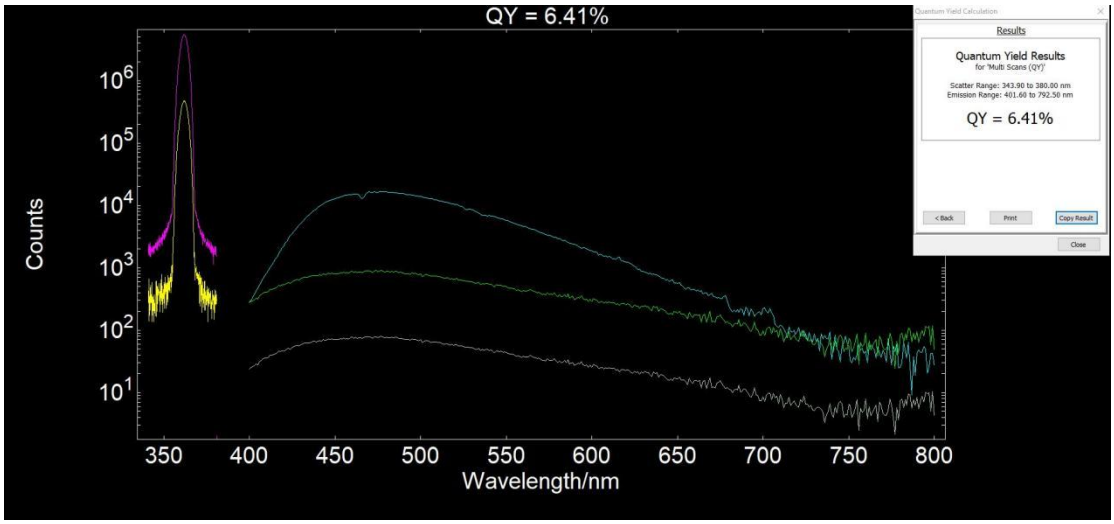

Fig. S16 Absolute fluorescence quantum yield of complex **2** in solid state.

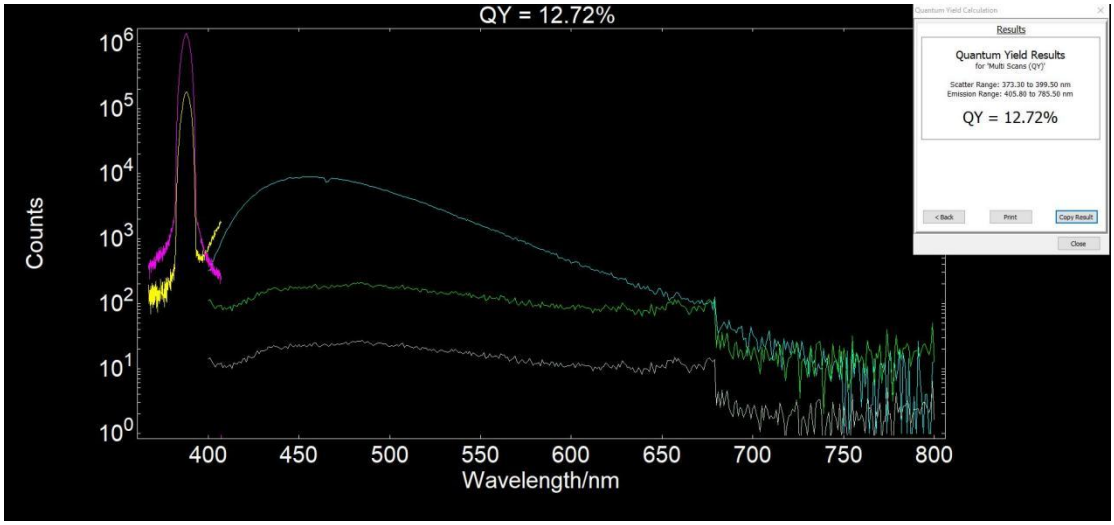

Fig. S17 Absolute fluorescence quantum yield of complex **3** in solid state.

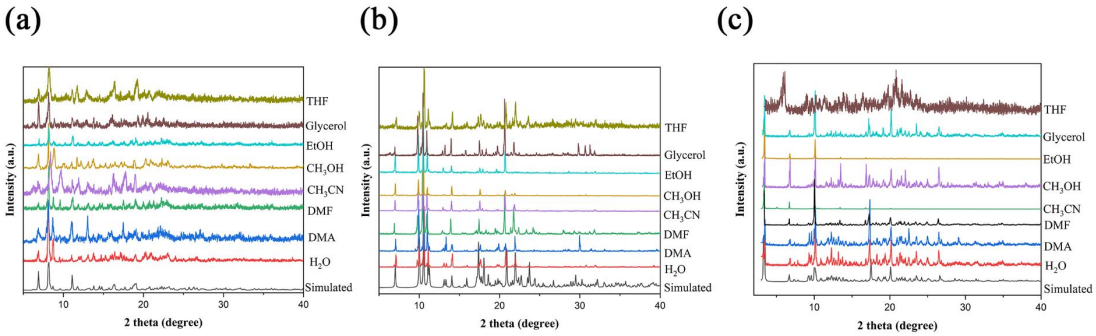

Fig. S18 PXRD powder patterns of complex **1** (a), complex **2** (b) and complex **3** (c) after treatment with different solvents.

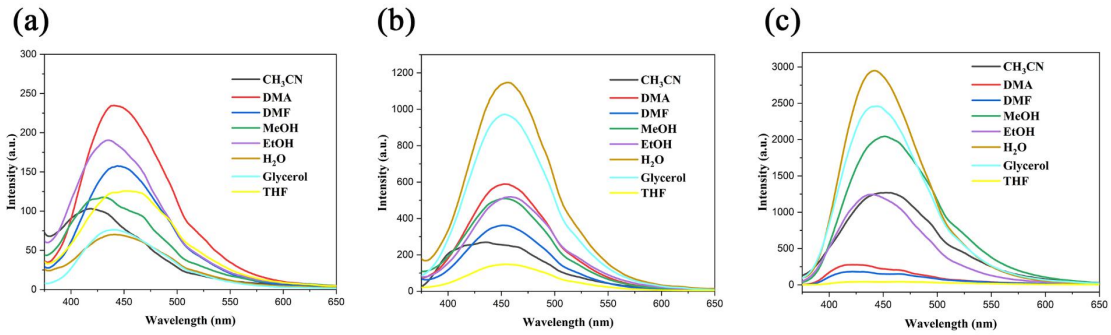

Fig. S19 Fluorescence spectra of complexes **1–3** dispersed in different solvents.

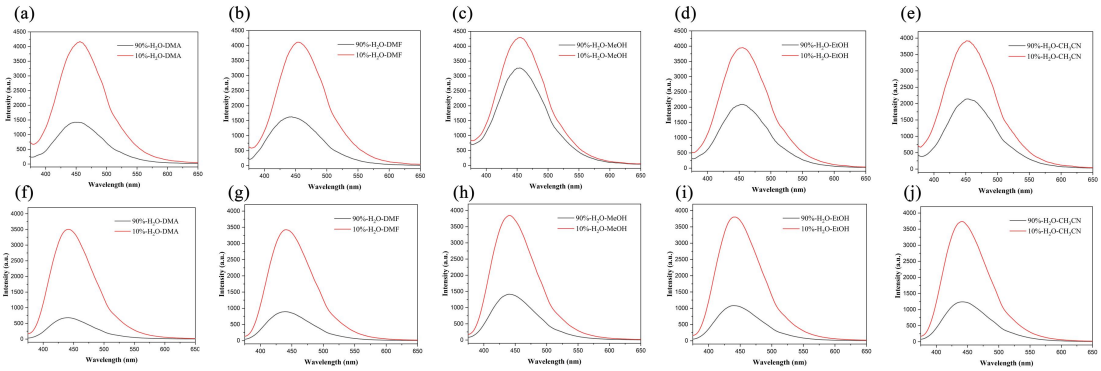

Fig. S20 Fluorescence spectra of complex **2** when the ratio of H_2O in different solvent systems is 90% and 10% (a-e) and fluorescence spectra of complex **3** when the ratio of H_2O in different solvent systems is 90% and 10% (f-j).

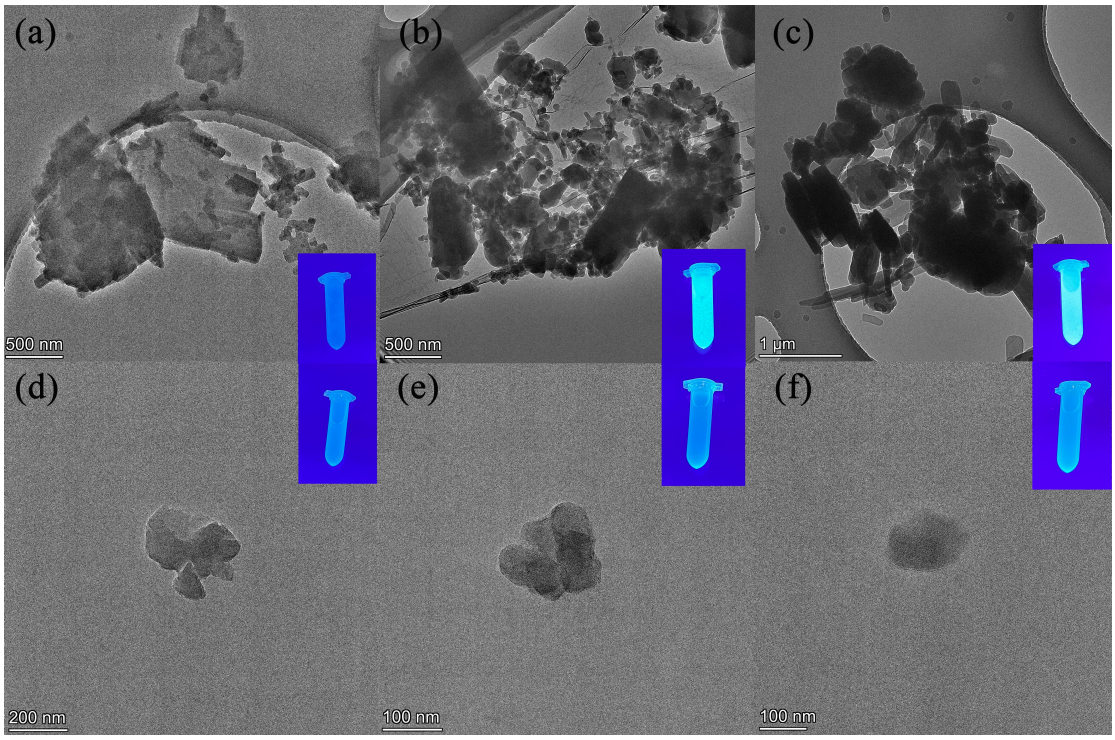

Fig. S21 The fluorescence photos under UV light and TEM images of complexes **1** (a), **2** (b) and **3** (c) in H_2O. The fluorescence photos under UV light and TEM images of complex **1** (d) in THF. The fluorescence photos under UV light and TEM images of complexes **2** (e) and **3** (f) in DMA.

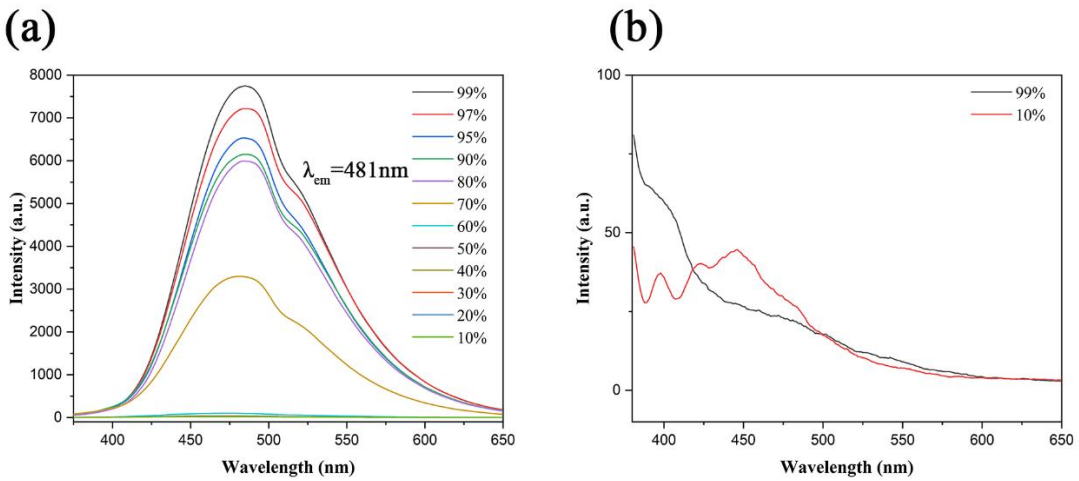

Fig. S22 Emission spectra of ligand tpemc (a) and ligand phen (b) in the DMA-H_2O solutions with different water volume fractions.

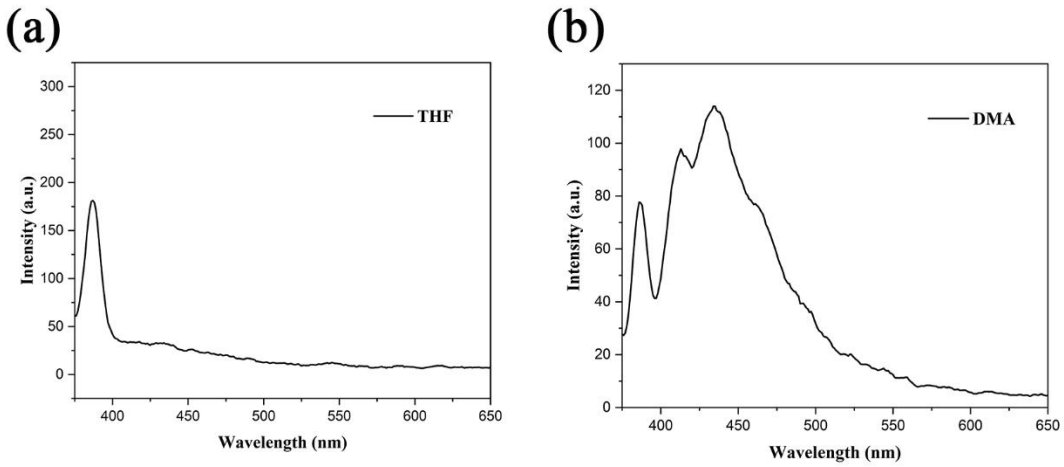

Fig. S23 (a) Fluorescence spectra of THF solvent (λ_{em}=387 nm), (b) fluorescence spectra of DMA solvent.

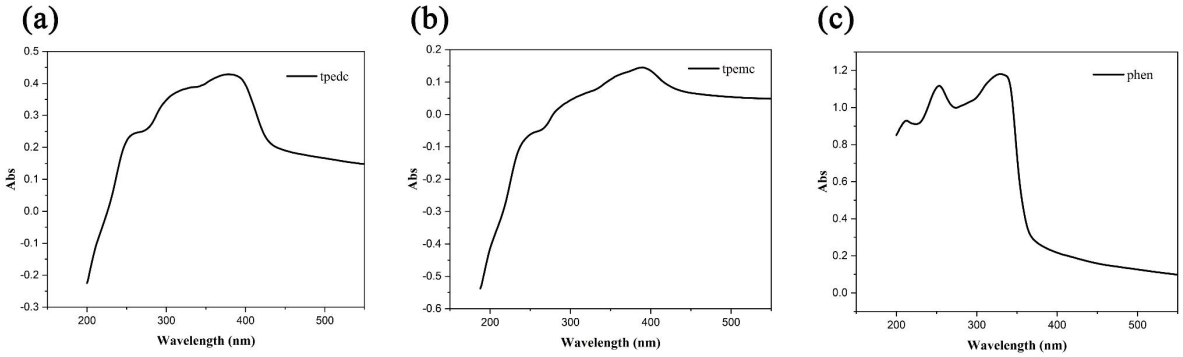

Fig. S24 UV-Vis absorption spectra of (a) tpedc, (b) tpemc and (c) 1,10-Phenanthroline monohydrate

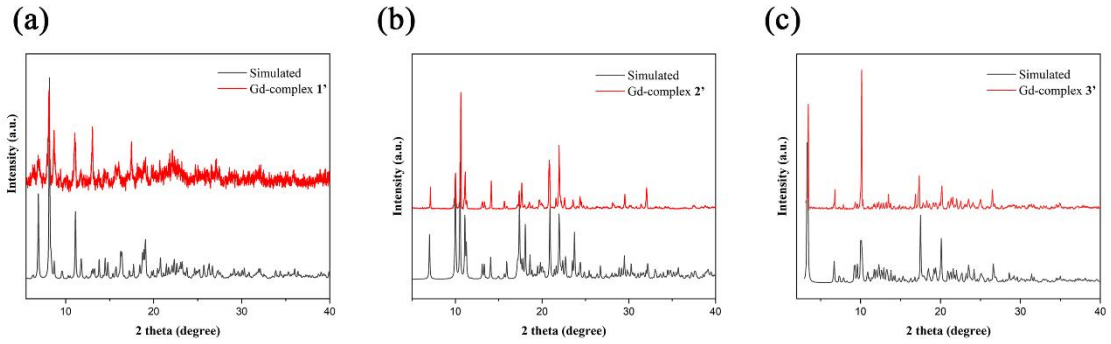

Fig. S25 PXRD patterns of Gd-complex **1'** (a), Gd-complex **2'** (b), and Gd-complex **3'** (c). Where the black line is obtained by software simulation (based structure of Eu-complex **1**–**3**), and the red line is the result obtained by the actual test of the Gd-complexes.

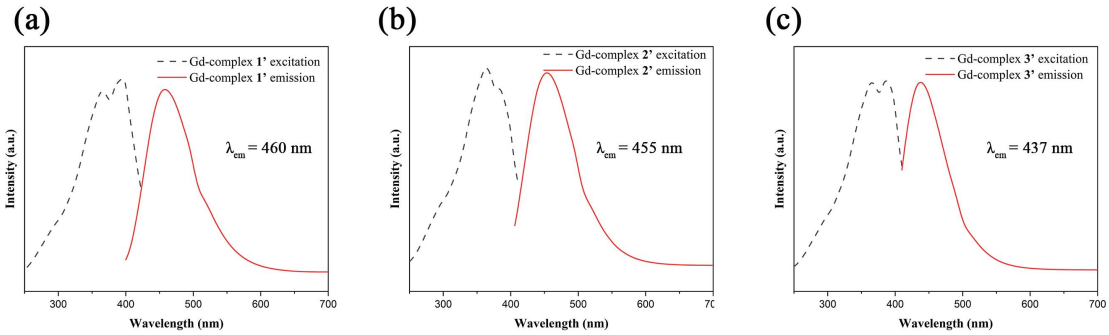

Fig. S26 Solid-state fluorescence excitation and emission spectra of Gd-complex **1'** (a), Gd-complex **2'** (b) and Gd-complex **3'** (c). The positions of emission peaks located at 460 nm, 455 nm and 437 nm, respectively. And the emission peak of ligands blue-shifted by 9 nm, 9 nm and 27 nm after forming the complexes.

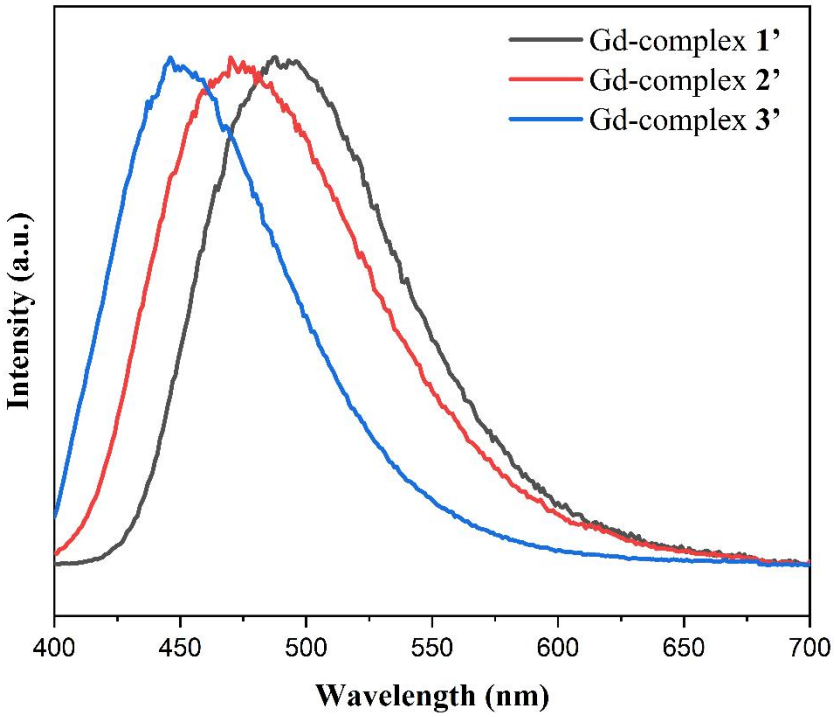

Fig. S27 The normalized phosphorescence spectrum of Gd-complex **1'**, **2'** and **3'** at 77 K, the phosphorescence emission peaks of Gd-complex **1'–3'** are 491 nm, 471 nm and 451 nm, respectively.

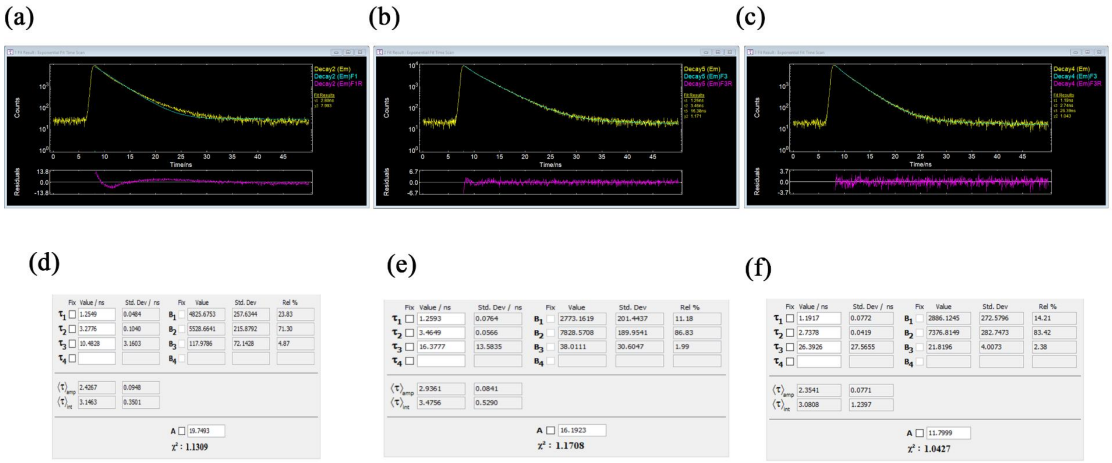

Fig. S28 Fluorescence lifetime of Gd-complex **1'** (a, d), Gd-complex **2'** (b, e) and Gd-complex **3'** (c, f). The lifetime was calculated to be 3.08 ns, 0.72 ns and 3.15 ns respectively.

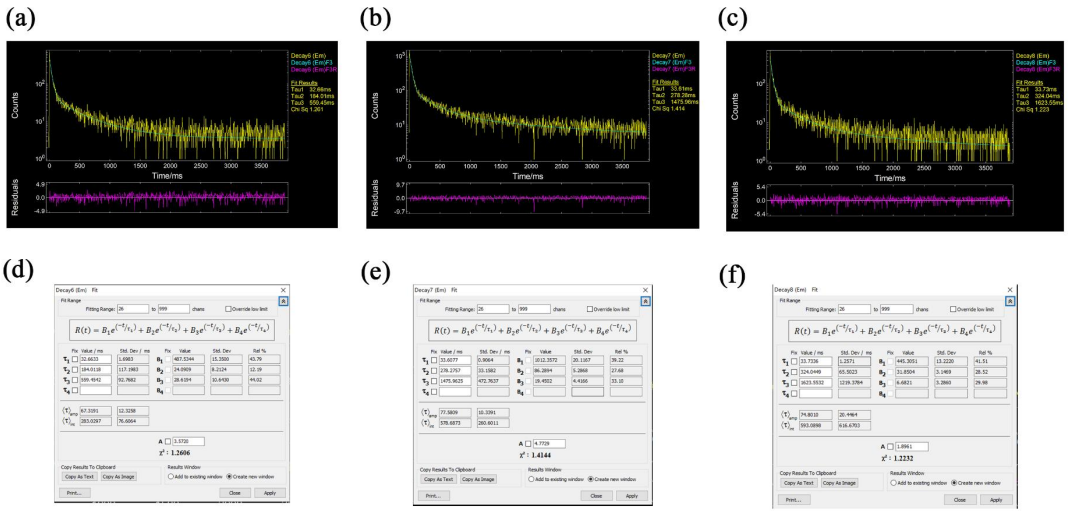

Fig. S29 Phosphorescence lifetime of Gd-complex **1'** (a, d), Gd-complex **2'** (b, e) and Gd-complex **3'** (c, f). The lifetime was calculated to be 283.00 ms, 578.75 ms and 593.16 ms respectively.

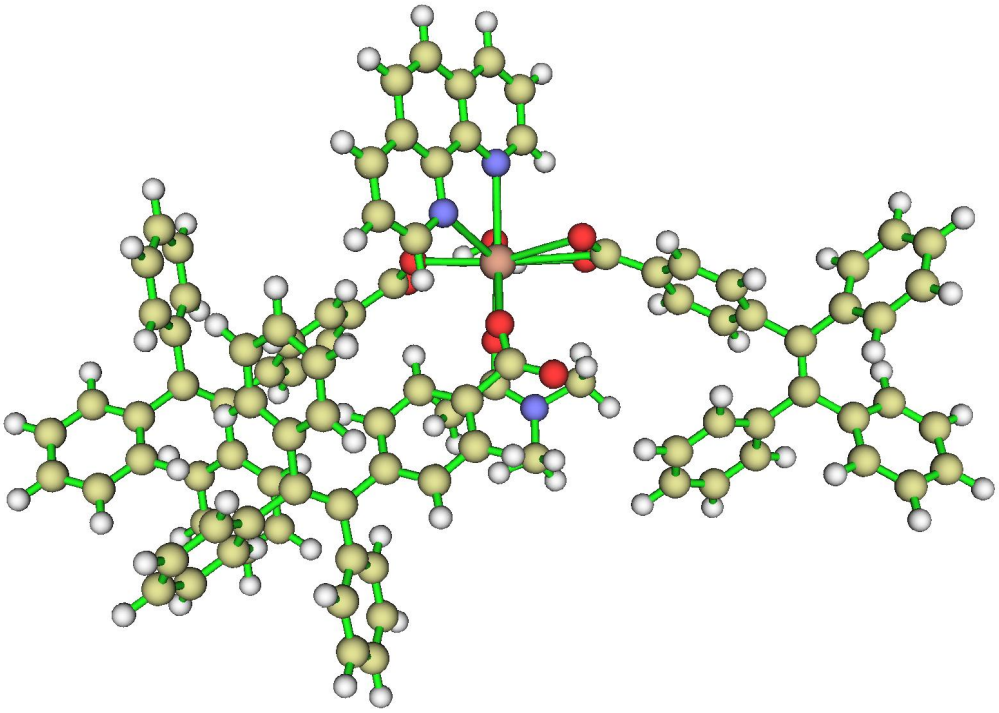

Fig. S30 Molecular representation of models of complex **3** employed for the calculations. Model consists of a representative excerpt of complex **3** in which the central Eu (Ⅲ) ion is surrounded by three tpemc ligands as well as one phen, a DMF molecule and a H_2O molecule in such a way that their original coordination environment is kept.

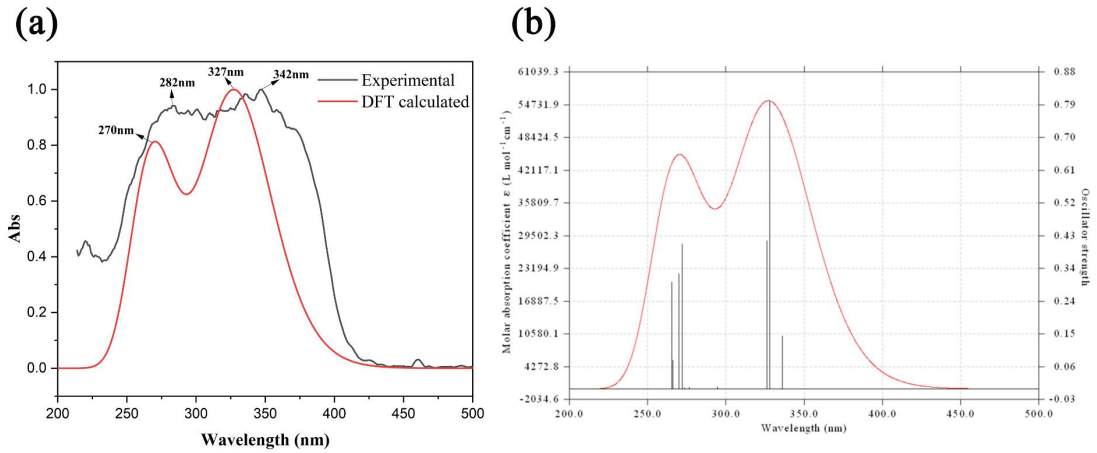

Fig. S31 (a) Comparison between experimental and calculated UV-vis absorption spectrum of the complex **3**, (b) calculated UV-vis absorption spectrum of the complex **3**.

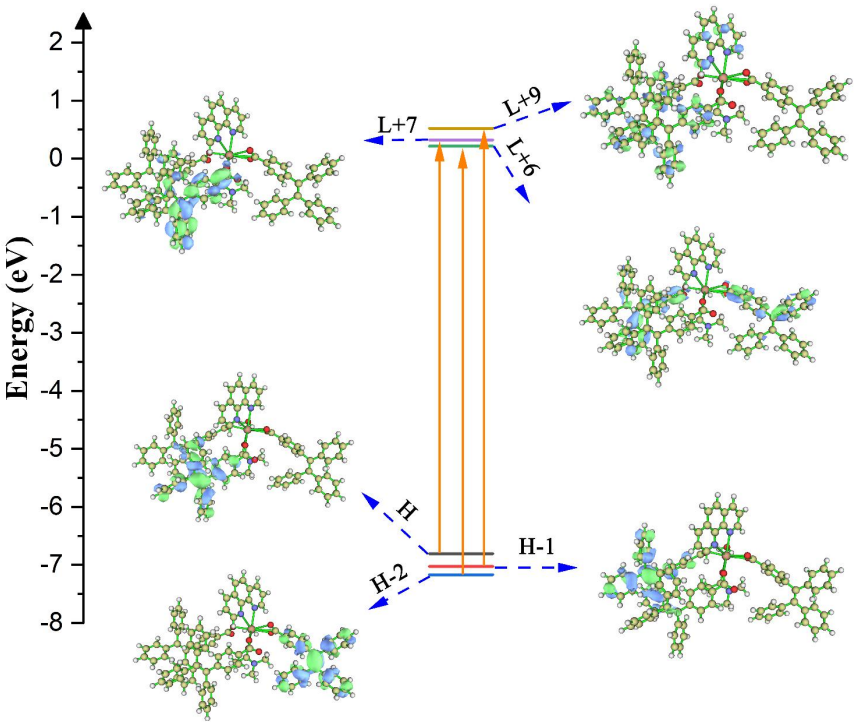

Fig. S32 Molecular orbital energy diagrams for complex **3** showing the vertical electronic transitions for the maxima absorption (270 nm) band at theoretical level when B3LYP/def2-TZVPP for C H O N and BLYP/ MWB52 for Eu.

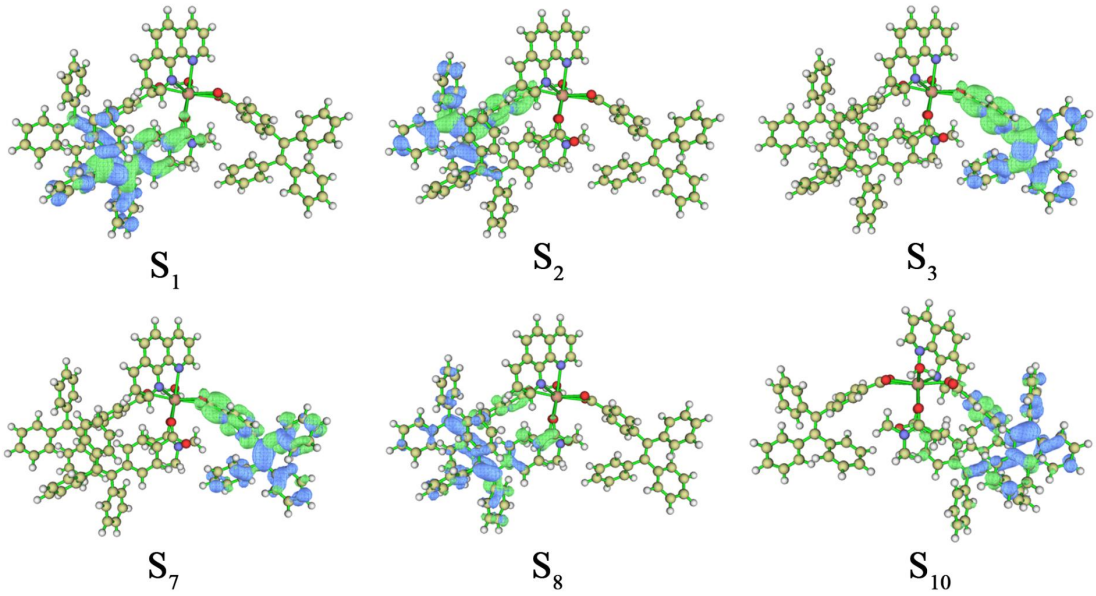

Fig. S33 Difference in electron density upon excitation from the ground S_0 state to the singlet excited state for complex **3**. Green and blue colors show regions of increasing and decreasing electron density, respectively. (Blue and green isosurfaces represent hole and electron distributions, respectively). And for the sake of simplicity only the six most significant absorptions have been selected.

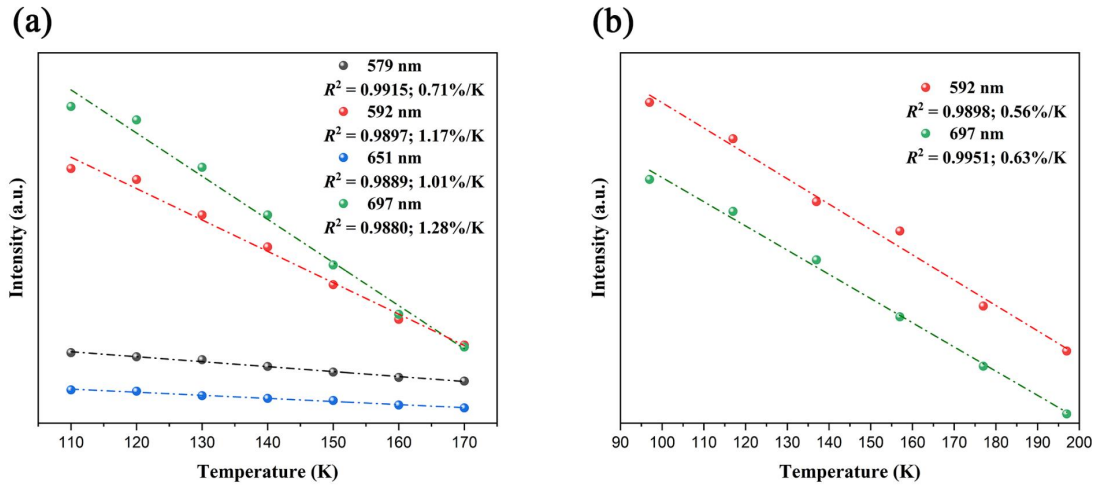

Fig. S34 Linear relationship between characteristic peak intensities (at different wavelength) and temperature of complex **2** (a) and complex **3** (b).

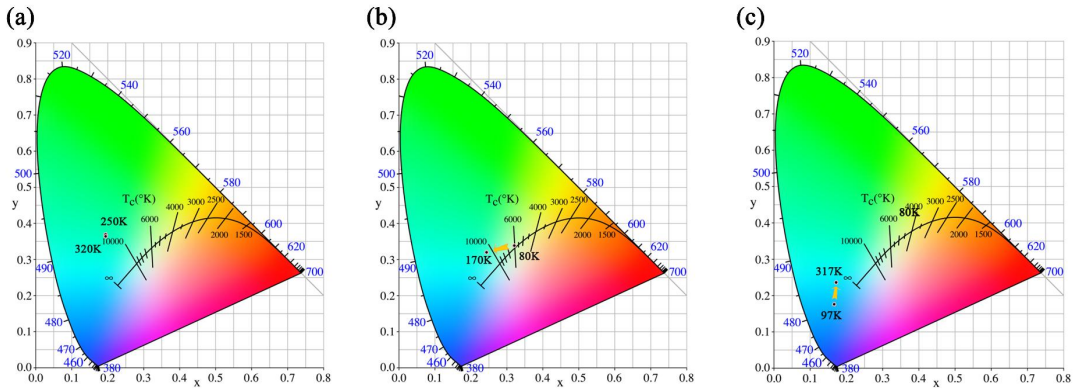

Fig. S35 CIE properties of complex **1** (a)， complex **2** (b) and complex **3** (c) under different temperature in solid state.

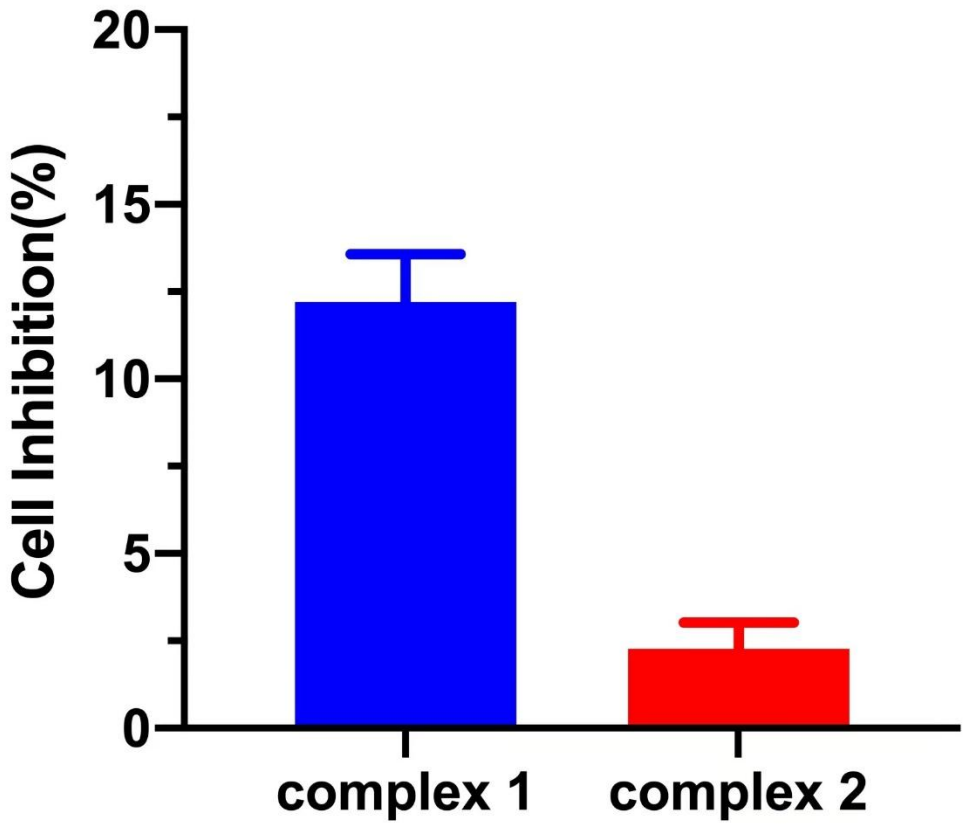

Fig. S36 Hela cell inhibition of complexes **1** and **2**.

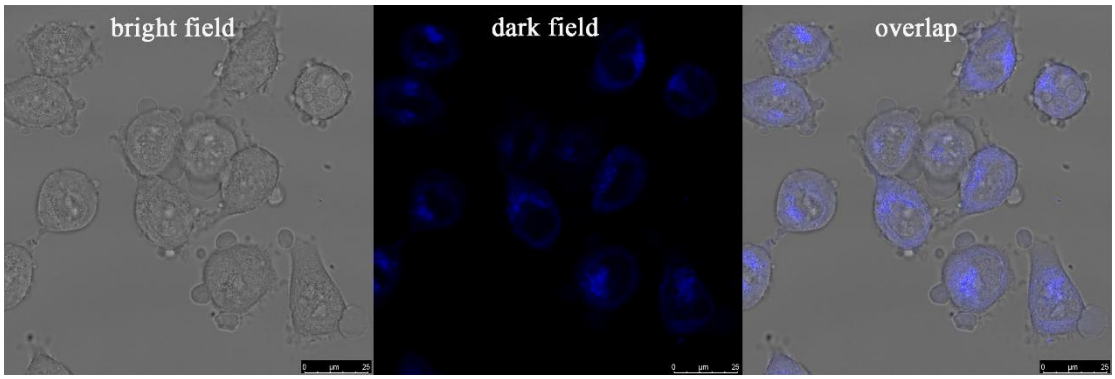

Fig. S37 Cell image of Hela cells with 0.2 μM complex **2** (bright field); cell image of Hela cells with 0.2 μM complex **2** (dark field); (d) overlap of the dark and bright field Hela cell images with 0.2 μM complex **2**.